Multi-step Molecular Docking and Dynamics Simulation-based Screening of Large Antiviral Specific Chemical Libraries for Identification of Nipah Virus Glycoprotein Inhibitors

Malti Sanjay Kalbhor[1#], Shovonlal Bhowmick[2#], Amer M. Alanazi[3], Pritee Chunarkar Patil[1], Md Ataul Islam[4,5*]

[1]*Department of Bioinformatics, Rajiv Gandhi Institute of IT and Biotechnology, Bharati Vidyapeeth Deemed University, Pune-Satara Road, Pune, India*
[2]*Department of Chemical Technology, University of Calcutta, 92, A.P.C. Road, Kolkata-700009, India*
[3]*Pharmaceutical Chemistry Department, College of Pharmacy, King Saud University, Riyadh 11451, Saudi Arabia*
[4]*Division of Pharmacy and Optometry, School of Health Sciences, Faculty of Biology, Medicine and Health, University of Manchester, Oxford Road, Manchester M13 9PL, United Kingdom*
[5]*School of Health Sciences, University of Kwazulu-Natal, Westville Campus, Durban, South Africa*
[6]*Department of Chemical Pathology, Faculty of Health Sciences, University of Pretoria and National Health Laboratory Service Tshwane Academic Division, Pretoria, South Africa*

[*]To whom correspondence should be addressed: ataul.islam80@gmail.com (MA Islam)

[#]Contributed equally and can be considered as the first author.

Highlights

- *Nipah Virus* (NiV) is highly lethal, emerging, and count among various medically important bat-borne viruses.
- A set of 79,892 compounds were screened against NiV protein through a multi-step molecular docking study.
- Based on Glide_XP score, binding free energy and pharmacokinetics assessment, 5 molecules found as potential NiV protein inhibitors.
- Binding interaction and molecular dynamics simulations suggested the potentiality of the selected molecules for NiV inhibition.
- •Binding energy calculated using MM-PBSA approach indicates strong binding affinity of the molecules towards NiV protein.

Abstract

Nipah virus (NiV) infections are highly contagious and can cause severe febrile encephalitis. An outbreak of NiV infection has reported high mortality rates in Southeast Asian countries including Bangladesh, East Timor, Malaysia, Papua New Guinea, Vietnam, Cambodia, Indonesia, Madagascar, Philippines, Thailand and India. Considering the high risk for an epidemic outbreak, the World Health Organization (WHO) declared NiV as an emerging priority pathogen. However, there are no effective therapeutics or any FDA approved drugs available for the treatment of this infection. Among the known nine proteins of NiV, glycoprotein plays an important role in initiating the entry of viruses and attaching to the host cell receptors. Herein, three antiviral databases consisting of 79892 chemical entities have been computationally screened against NiV glycoprotein (NiV-G). Particularly, multi-step molecular docking followed by extensive molecular binding interactions analyses, binding free energy estimation, *in silico* pharmacokinetics, synthetic accessibility and toxicity profile evaluations has been carried out for initial identification of potential NiV-G inhibitors. Further, molecular dynamics (MD) simulation has been performed to understand the dynamic properties of NiV-G protein-bound with proposed five inhibitors (G1-G5) and their interactions behavior, and any conformational changes in NiV-G protein during simulations. Moreover, Molecular Mechanics Poisson-Boltzmann Surface Area (MM-PBSA) based binding free energies (ΔG) has been calculated from all MD simulated trajectories to understand the energy contribution of each proposed compound in maintaining and stabilizing the complex binding interactions with NiV-G protein. Proposed compounds showed high negative ΔG values ranging from -166.246 to -226.652 kJ/mol indicating a strong affinity towards the NiV-G protein.

Keywords: Nipah virus glycoprotein, Molecular docking, Molecular dynamics, MM-GBSA / MM-PBSA, Virtual screening

Graphical abstract

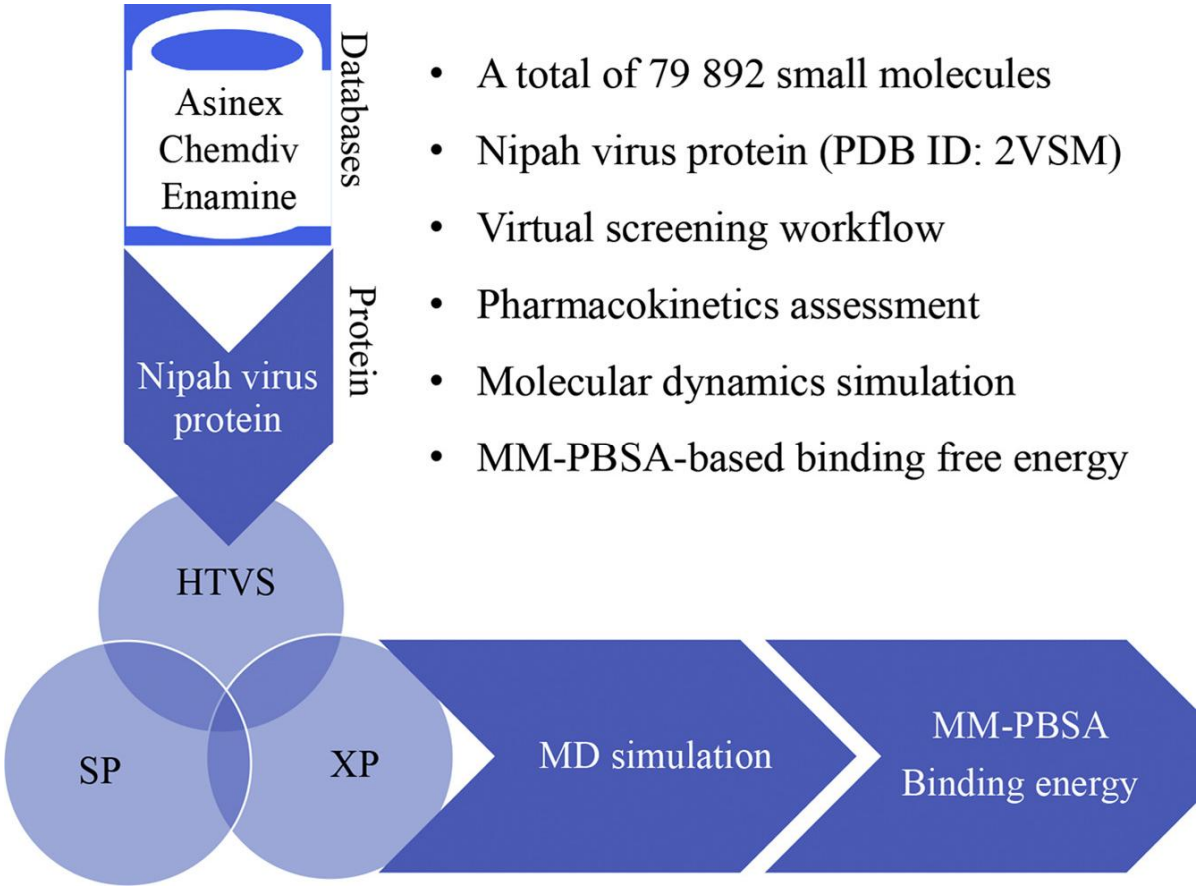

1. Introduction

Nipah Virus (NiV) belongs to the family *Paramyxoviridae*, leading as highly lethal, emerging, and count among various medically important bat-borne viruses that can infect humans directly or via domestic animals [1, 2]. It has been reported that genetic features of various paramyxoviruses are retained by NiV and thereby it might also hold back similar types of biological actions as well [3, 4]. NiV is a zoonotic virus and it first appeared in domestic pigs in Malaysia and Singapore in the year 1998 and 1999 [5-7]. The virus was originally discovered in Sungai Nipah village in Malaysia and thereby it is named NiV. According to the report of the World Organization for Animal Health (https://www.oie.int/en/animal-health-in-the-world/animal-diseases/Nipah-Virus/), the NiV infection was noted in the human body in Bangladesh and India in the years of 2003, 2004, 2007 and 2008 without any related domestic animal outbreaks. In time, NiV has majorly caused outbreaks in Asian countries including

Indonesia, Cambodia, Papua New Guinea, Vietnam, Philippines and Thailand [8]. In 2018, as a leading cause of emerging zoonotic disease, NiV was listed as a high priority pathogen by World Health Organization (WHO) (https://www.who.int/news-room/fact-sheets/detail/nipah-virus). In the Kerala province of India, the NiV infection outbreak was reported in May 2018 and that led to the death of 17 individuals [9]. Although NiV infection poses severe encephalitis and consider as a great threat to public health, however, there are no effective vaccines or antivirals are commercially available. Such severe encephalitis can often lead to serious febrile illnesses with neurological disorders [9]. Though NiV infections are highly contagious, however, since it first outbreaks the research studies on NiV have been largely neglected. NiV enters into the host systems (either human or animals) through the oro-nasal routes and supposed to replicate in lymphoid and respiratory tissues for causing infections [10, 11].

The NiV genome is a negative-sense single-stranded RNA extend around 18.2-kb nucleotides, comprises 6 genes, which ultimately encodes 6 structural proteins namely the Nucleocapsid protein (N), Phosphoprotein (P), Matrix protein (M), Fusion protein (F), Glycoprotein (G) and Large polymerase protein (L) in the order 3´-N-P-M-F-G-L-5´. P gene encodes three more proteins C, V and W which are non-structural proteins [10, 11]. Among six structural proteins of NiV, N, P and L proteins are attached with the viral RNA forming the virus ribonucleoprotein (vRNP). G and F proteins play important roles while NiV entering into the host cell. A very important aspect to note here that NiV-G protein is responsible for cellular or host attachments by means of interacting with the host cell surface receptors such as ephrin B2 or B3 [10, 11]. Ephrin-B2 is expressed on endothelial cells, smooth muscle cells and neurons, and acts as a cellular receptor of NiV [10-13]. NiV infection spread through the two most important target cell types: epithelial and endothelial cells. *In vivo* infection occurs via cell-to-cell fusion which is largely mediated by NiV glycoproteins [12]. Therefore, targeting to block the active functional domain of NiV-G protein or by modulating or inhibiting the NiV-G protein function by a small molecule can facilitate the development of an efficient vaccine or antiviral drugs for prevention or treatment of this highly neglected NiV infection. It is well-established fact that NiV-G plays a key role in viral entry with the response to host cell surface receptors ephrin B2. Therefore, it can be postulated that blocking the region of NiV-G protein or specific NiV-G protein residues involved in the formation of interactions with ephrin B2 will hamper the viral attachment or cell-to-cell fusion and hence restriction in viral entry into the host cell can be

achieved. Earlier, the specificity of few NiV-G protein residues (Tyr581and Ile588) in the active site or binding pocket has been demonstrated to be catalytically very important residues in terms of contributing hydrophobic interactions that can accommodate host cell ephrin B2 receptor residues [14]. Accounting for such considerations, structural information of NiV-G protein can be used as a potential template for structure-based drug design.

Hence, for the development of antiviral drug-like candidates of NiV, a computationally exhaustive multi-step molecular docking based virtual screening technique has been employed on three specific large antiviral chemical libraries. Moreover, the screening protocol also includes step-by-step filtration of compounds through absorption, distribution, metabolism, and excretion (ADME) and toxicity profile analyses. Further, long-range 100 ns molecular dynamics (MD) simulations analysis combined with Molecular Mechanics Poisson-Boltzmann Surface Area (MM-PBSA) based binding free energies have been estimated for finally selected five proposed compounds (G1 – G5) which exhibited high negative binding free energies ranging from -166.246 to -226.652 kJ/mol. Therefore, the conducted study findings provide valuable insight into the possible mechanistic interactions of NiV-G protein with five selected promising compounds for developing novel antiviral drugs to control the NiV infection.

2. Materials and Methods

2.1 Collection and preparations of antiviral compound libraries

Three different chemical library databases specifically containing the antiviral specific chemical entities were collected from publicly available sources or on request. All three antiviral chemical databases *viz*. Asinex-Antiviral Library (http://www.asinex.com), Enamine-Antiviral Library (www.enamine.net) and ChemDiv-Antiviral Library (www.chemdiv.com) were downloaded in .sdf format. Altogether, a total of 79,892 chemical entities (i.e. Enamine - 3700, Asinex - 8722, and ChemDiv - 67470) were collected from these three databases. Each antiviral database has met the growing need for effectively designing and screening out selective antiviral agents to expedite the modern drug discovery research and is also used in a wide range of antiviral drug discovery projects. Moreover, each selected antiviral database is comprised of compounds having attractive drug/lead-like physicochemical and structural properties and is also considered to be a good or convenient starting point for antiviral therapeutics development.

Prior to use in modeling purposes, all compounds collected from three databases were prepared to employ LigPrep module [15] in Meastro interface of Schrödinger suite. Particularly, ligand preparation was carried out using LigPrep for generating the most possible library of ligand conformers for each compound which can be easily and readily used during protein-ligand docking to assess the ligand flexibility. For executing the LigPrep module, mostly all default parameters were selected except a maximum of nine numbers of stereoisomers were allowed to generate for each compound. For all compounds, possible ionization states were achieved at an assigned pH range of 7.0±2.0. The 3D molecular structure with low-energy conformers was generated after the successful execution of LigPrep for each ligand employing Optimized Potentials for Liquid Simulations (OPLS3) force field [16].

2.2 Nipah virus glycoprotein (NiV-G) structure selection and preparation

Among the several NiV-G crystal structures available in the Protein Data Bank (PDB) [17], the NiV-G complex with human cell surface receptor ephrin B2 was retrieved (PDB ID: 2VSM) [18] for subsequent modeling purposes. Such selection was made based on the submitted experimental resolution and R-value of the crystal structure. It was noted that among all deposited NiV-G crystal structures in PDB, the PDB ID: 2VSM had the best experimental resolution of 1.80 Å and hence selected.

To prepare the selected protein structure, all non-protein entities like water molecules and other small molecules attached to the crystal structure were removed. Using the "Protein Preparation Wizard" module [19], the NiV-G was prepared following standard protocols like assignment and optimization of bond order and length, creation of disulfide bonds, terminals capping of protein with ACE and NMA residues, and fixing of any missing side chains. For Asp, Glu, Arg, Lys and His amino acid residues, possible tautomeric states were achieved and protonation of the protein structure was generated [20]. In addition, during the protein preparation step, hydrogen atoms were added and subsequently optimized the hydrogen bonds as well. Restrained minimization was further carried out applying OPLS3 force field to achieve energy minimized protein structure until the root mean squared deviation (RMSD) reached to 0.3 Å.

2.3 Grid preparation for NiV-G

For setting up the grid generation job, the 'Receptor Grid Generation' module of Schrödinger suite (Schrödinger, 2018) was used. The grid generation was executed ensuring that residues Gln559, Glu579, Tyr581, and Ile588 and other consecutive residues in close proximity were appropriately enclosed inside the specified rectangular grid box. The above-mentioned residues showed high binding interactions affinity towards ephrin B2 [14, 21], hence the grid was generated around these residues. Therefore, specifying X, Y, and Z cartesian coordinates (X=16.09, Y=70.13 and Z=-24.49 Å) grid generation job was executed. During grid generation, no specific positional constraints were set or defined. After successful completion of grid job generation, the grid file was created which represents the active site information of NiV-G protein and kept until further used in docking procedure.

2.4 Structure-based virtual screening of antiviral dataset using multi-step docking

An extensive and rigorous hierarchical molecular docking-based virtual screening (VS) protocol was used to screen out three antiviral chemical libraries downloaded from Asinex, ChemDiv and Enamine databases. All three chemical library databases were hierarchically filtered out following Glide-high-throughput virtual screening (HTVS), standard precision (SP), and extra precision (XP) docking protocol employing the "Virtual Screening Workflow" (VSW) utility module integrated into the Schrödinger suite [22]. In particular, three different docking protocols namely HTVS, SP and XP were executed under a specific set of parameters assigned in the VSW tool. Under 'Input' tab all prepared chemical compounds libraries were browsed, and subsequently, under the 'Filtering' tab 'QikProp' run option was selected in order to get the most potential drug-like compounds to be pre-filtered. In the 'Preparation' tab no further preparations of compounds were allowed. The prepared NiV-G receptor grid file was browsed under 'Receptor' tab. Finally, the 'Docking' tab job was assigned as top 10% of best-docked compounds to be retained in both HTVS and SP docking, followed by top 50% compounds to be retained in Glide-XP docking step for further processing. Finally, XP-descriptor information was written for all best scoring NiV-G-ligand complexes. Further, all retained NiV-G-ligand complexes were post-processed for estimating binding free energies following the Prime-MM-GBSA method. The entire virtual screening workflow protocol was executed in the CHPC server (https://www.chpc.ac.za/index.php/resources/lengau-cluster), Cape Town, South Africa. After

successful completion of the virtual screening procedure, the user-defined cut-off XP dock score and MM-GBSA score were used to reduce the chemical space and remaining compounds considered for the next level of assessment.

2.5 In silico ADME and toxicity properties prediction

The pharmacokinetics profile assessment was carried out for the retained VSW based screening molecules. The SwissADME [23], a web-server based open-source tool was used for ADME profile prediction for all compounds. A number of physiochemical, lipophilicity, water-solubility, drug-likeness and medicinal chemistry properties including Lipinski's rule of five (LoF) and Veber's rule were estimated. All these properties were examined to select the best potential NiV-G inhibitor identifications among the set of studied compounds. Further, molecules that fulfilled the above criteria were subjected to toxicity properties prediction. Some toxic and environmental effects of each molecule was checked through the 'TOxicity Prediction by Komputer Assisted Technology' (TOPKAT) module embedded in Discovery Studio Client (version 2020) of BIOVIA Inc. Particularly, TOPKAT module used to check the chemical features and compared those data with available toxicological endpoints which already been experimentally established and finally predicted the parameters such as carcinogenicity, mutagenicity, toxicity, irritant or developmental toxicity, etc. All ADMET properties calculated are quite important in pharmaceutical and drug developmental research for evaluating and reducing the number of safety issues usually checked during the drug discovery application.

2.6 Molecular dynamics simulations and binding free energy estimations by MM-PBSA method

In order to assess the stability and dynamic behavior of proposed NiV-G protein-ligand complexes, a long-range 100 ns MD simulation was carried out using Groningen Machine for Chemical Simulation (Gromacs 2018.2) software tool (http:// www.gromacs.org/) [24, 25] installed at Lengau CHPC server (https://www.chpc.ac.za/index.php/resources/lengau-cluster).

The time step, constant temperature and constant pressure were adopted as 2 fs, 300 K and 1 atm, respectively. The protein topology was generated using the CHARMM36 force field. The ligand topology was calculated using the online server, the SwissParam. Each NiV-G protein-ligand complex was confined within a cubic box of 100 x 100 x 100 $Å^3$. Moreover, the

complex was centered in the specified cubic box and the minimum distance maintained as 10 Å between the atoms of protein-ligand complex and the box edge. The TIP3P water model was used to solvate the system [34]. In order to neutralize the system, the required number of Na^+ and Cl^- ions were adjusted. Thereafter, exhaustive energy minimization was performed for each of the NiV-G protein-ligand complex systems and followed by simulation production executed. The close-contacts or overlaps between the atoms were addressed by the steepest descent algorithm. The system was equilibrated with NVT (constant number of particles, volume and temperature) as well as NPT (constant number of particles, pressure and temperature) to ensure the equal distribution of solvent and ions around the protein-ligand complex in the system. To analyze the conformational changes and stability of the protein-ligand system, several parameters such as RMSD, root mean square fluctuation (RMSF) and radius of gyration (RoG) were calculated.

After the successful production of MD simulations run of each NiV-G protein-ligand complex, all trajectories data of MD simulation was utilized to estimate the binding free energies using MM-PBSA (Molecular Mechanics Poisson-Boltzmann Surface Area) method employing g_mmpbsa utility tool [26]. The detailed mathematical formula for the derivation of binding free energies using MM-PBSA procedure can be found in our previous publications [27-29].

3. Results and discussion

3.1 Virtual screening analyses

In recent days, structure-based virtual screening (SBVS) is a commonly used computational approach and implemented towards the discovery of novel and selective molecules for inhibiting or modulating specific bioactive target macromolecules [28, 30-33]. In the research-based pharmaceutical industry, the uses of three dimensional (3D) bioactive targets have increasingly engaged in the SBVS or medicinal chemistry techniques with the integration of *in silico* and experimental methods. Efforts are being given towards an up-to-date understanding of the intricate aspects of inter- or intra-molecular recognition and optimization. Striking advancement and progress in structural or molecular biology studies have enabled us to solve more than a hundred thousand 3D protein structures across several kingdoms. Among the solved 3D protein structures, a number of targets have received great priority to be the key macromolecular drug targets for many diseases [33]. Within this framework, although a conventional but rigorous SBVS technique has been employed in the present study intended to identify potential small

molecules from three different antiviral databases *viz.* Asinex, ChemDiv and Enamine screened against the NiV-G protein through the multi-cheminformatics approaches. The flow diagram of the presently employed work for the identification of small molecular chemical entities for NiV-G protein is given in Figure 1.

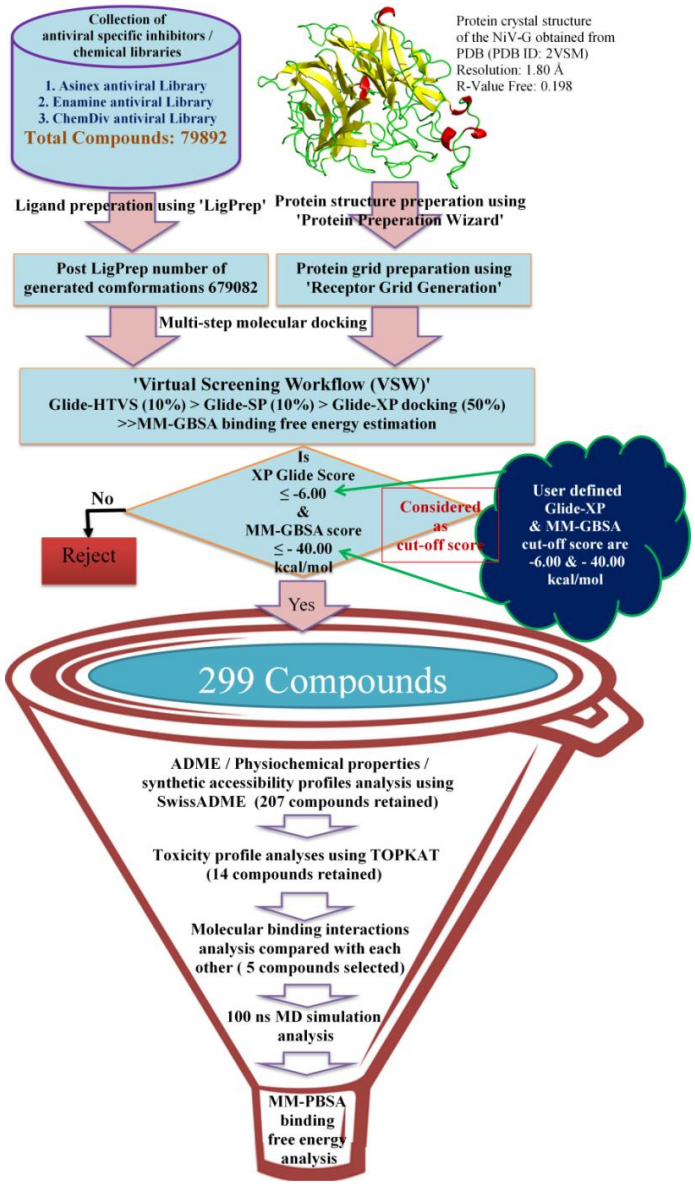

Figure 1. Schematic workflow of the virtual screening procedure for identification of promising inhibitors/modulators of NiV-G protein

In the present study, initially an extensive multi-step molecular docking and followed by binding free energy assessment by Prime–MM-GBSA approach have been implemented against

79892 chemical entities. In particular, multi-step molecular docking including Glide-HTVS, Glide-SP and Glide-XP have been performed to screen out best docking scores compounds binds to NiV-G protein. Almost 50% of compounds have been manually inspected for XP dock score and MM-GBSA score. It has been revealed that XP dock score and MM-GBSA score are ranging from -6.69 to -1.86 Kcal/mol and -52.96 to -26.71 Kcal/mol, respectively as per VSW generated outcomes. Further based on user-defined cut-off score (XP dock score as -6.00 kcal/mol and MM-GBSA score as -40.00 kcal/mol), a total of 299 compounds have been selected for subsequent analyses. Such a user-defined cut-off score is completely unbiased, rather targeted or assumption made to get the best score compounds with better binding potentiality. Preliminary, few lowest and highest XP dock and MM-GBSA scored compounds have been manually investigated for their molecular interactions and binding orientations analyses at the active site cavity of NiV-G protein. Such inspection has suggested that higher XP-dock and MM-GBSA score compounds are lacking the hypothesized scientific vision. It has been revealed that the higher XP-dock and MM-GBSA scored compounds showed a different kind of binding orientations (such as posed as off-target binding) as well as a higher number of binding interactions. Therefore, prior attention has been given to compounds that are bound at the nearer to the active site of the NiV-G protein. Further, *in-silico* pharmacokinetic studies including ADME and synthetic accessibility properties analyses have been performed on all 299 compounds to explore drug-likeness parameters. A total of 207 compounds have been found to adjudge good absorption, distribution, metabolism and excretion profiles, and drug-likeness characteristics. Thereafter, TOPKAT based toxicity prediction assessment resulted in 14 non-toxic compounds with accepted drug-like profiles. Further, in order to narrow down the chemical space, their molecular binding modes and intermolecular interactions have been critically checked which led down to the final selection of the best five compounds as NiV-G protein inhibitors/modulators. 2D chemical representation of all proposed compounds is depicted in Figure 2.

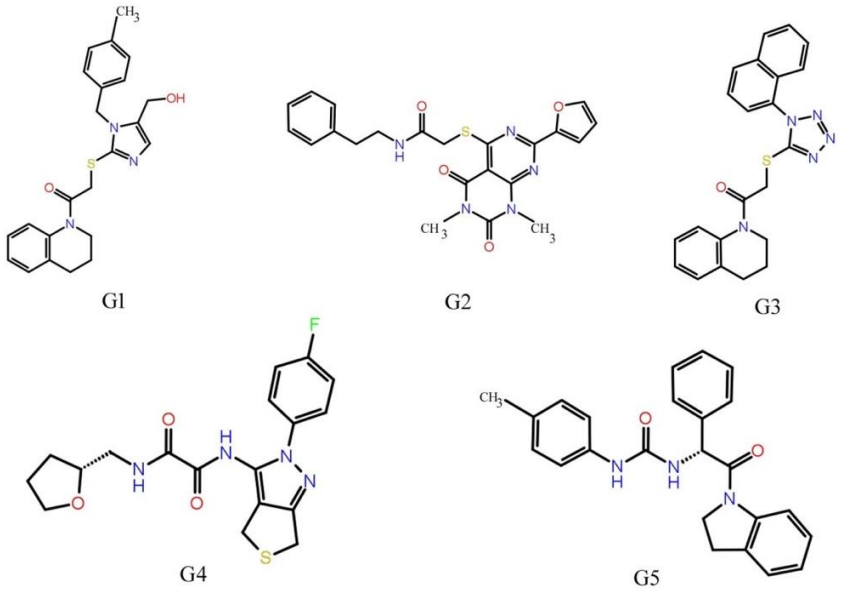

Figure 2. 2D representation of chemical structures of selected compounds identified as potent NiV-G protein inhibitors/modulators

3.2 Molecular docking based interaction analyses between NiV-G protein and identified inhibitors/modulators

In order to a deep exploration of molecular binding interaction analyses of NiV-G protein and identified inhibitor complexes obtained through the XP-docking method, the Protein-Ligand Interaction Profiler (PLIP) [34] tool was used. A number of molecular interactions such as hydrophobic interactions, hydrogen bonds, π-cation and π-stacking, etc. were detected between the NiV-G protein and newly identified ligand inhibitors. Results of molecular binding interaction profiles of all five compounds are presented in Table 1 and 3D interactions plot is displayed in Figure 3. In particular, compound G1 shows several numbers of hydrophobic interactions with atoms of Pro441, Pro488, Val507, and Lys560 amino acid residues and hydrogen bond (H-bond) interactions with residues Trp504 and Tyr508 of NiV-G protein. In addition, another two residues, Phe458 and Trp504 have also participated in π-stacking interactions with compound G1. In the case of G2, mostly hydrophobic contacts have been noticed with amino acid residues Pro441, Glu505A and Val507, and along with a π-cation interaction (distance 2.96 Å) with basic the amino acid residue, Lys560.

Table 1. Glide-XP dock, MM-GBSA scores and interacting residues of NiV-G protein with proposed five identified inhibitors.

Compounds	Glide XP / MM-GBSA score (Kcal/mol)	Interacting residues in H-bond interaction	Other type of molecular interactions
G1	-6.56 / -52.45	Trp504, Tyr508	Pro441, Pro488, Val507, Lys560 (Hydrophobic) / Phe458, Trp504 (π-Stacking)
G2	-6.45 / -50.12	Arg236, His281, Tyr508	Pro441, Glu505, Val507 (Hydrophobic) / Lys560 (π-Cation)
G3	-6.24 / -50.86	Cys240, Ser241, Gln559	Ala532, Gln559, Glu579, Tyr581, Ile588 (Hydrophobic)
G4	-6.07 / -44.12	His281, Tyr508, Lys560	Phe458, Trp504 (Hydrophobic)
G5	-6.39 / -46.92	Gln559	Val507, Gln559, Glu579, Ile588 (Hydrophobic) / Tyr581 (π-Stacking)

Compound G2 has also been formed several numbers of H-bond interactions with different amino acid residues namely Arg236, His281 and Tyr508. The Arg236 residue of NiV-G protein has been found to form two H-bond interactions with distance measured as of 2.12 and 2.06 Å. Compound G3 has two naphthalene rings at the terminal region mostly mediated the formation of hydrophobic interactions with Ala532, Gln559, Glu579, Tyr581 and Ile588 residues, whereas pentazolidine present as the linker substance participated to form H-bond interactions with residues Cys240, Ser241 and Gln559 of NiV-G protein. For compound G3, all H-bond and hydrophobic interactions are measured within the distances of 1.89 – 2.87 Å and 2.16 – 3.02 Å, respectively. From the binding interaction analysis of compound G4, it has been revealed that two amino acid residues, Phe458 and Trp504 of NiV-G protein participated to form hydrophobic interactions with measured distances of 3.02 and 2.69 Å, respectively. The presence of two carbonyl groups in G4 helped in the formation of H-bond interactions with two basic amino residues His281 and Lys560. In addition to the above, amino acid residue Tyr508 has also been found to form another H-bond interaction with the methoxy group of G4. In the case of G5, single amino residue Gln559 has been found to form a total of three H-bond interactions (distances measured within the ranges of 2.06 – 2.76 Å). The hydrophobic interactions have been observed with Val507, Gln559, Glu579, Ile588 of NiV-G protein and G5. In addition, a π-stacking interaction has also been observed with G5 and Tyr581 residue of NiV-G protein.

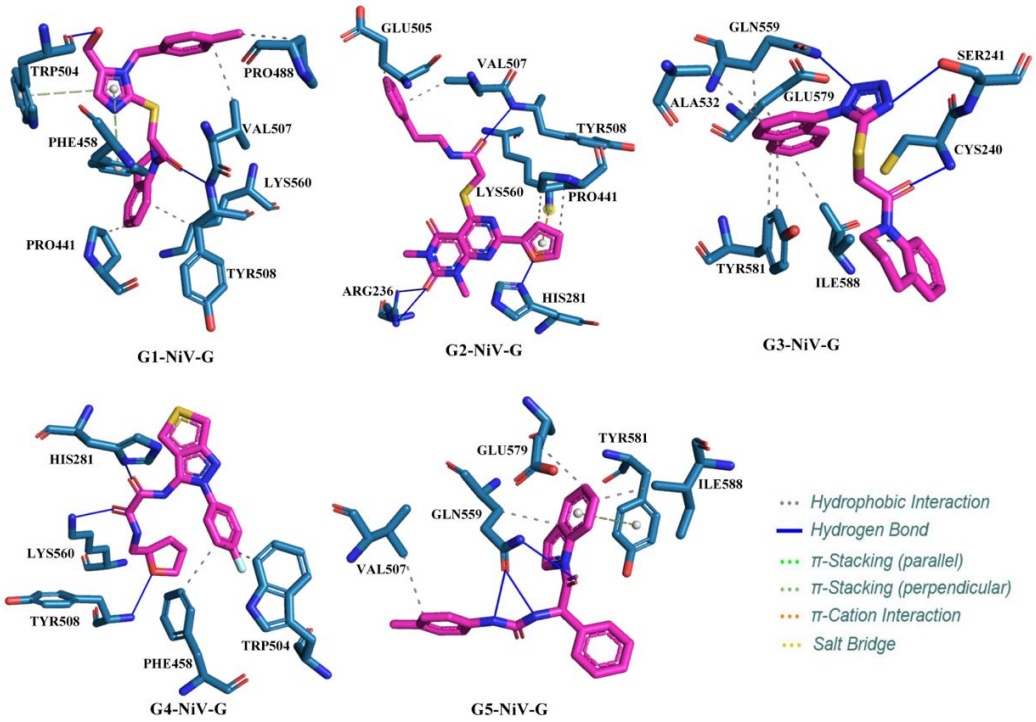

Figure 3. 3D representation of molecular binding interaction plot of selected five compounds identified as potent NiV-G inhibitors/modulators

Overall, from the docking interactions analyses, it has been revealed that residue Tyr508 of NiV-G protein as a common key residue associated with the formation of H-bond interactions with several compounds identified in this study. On the other hand, few other catalytically important NiV-G protein residues such as Val507, Lys560, Gln559, Glu579, Tyr581 and Ile588 have also been found to be common residues that participate in hydrophobic interactions with G1, G2, G3, and G5. These residues of NiV-G protein play critical roles by means of allowing further accommodation with the host cells receptor proteins [14, 18, 21]. Therefore, any kind of interaction with these residues is very crucial in terms of restricting any further interactions with the host cells receptor proteins. Moreover, the presence of several suitable functional groups in identified proposed compounds has enhanced the chance of creation of potential binding interactions with other close proximity amino acid residues in the active site of the NiV-G protein that might also trigger some induce fit effect to the NiV-G protein, and hence to exhibit biologically desirable outcomes. Figure 4 displayed the binding orientation of the proposed compounds and how each compound perfectly fitted inside the receptor cavity of NiV-G protein.

Each compound has been detected to be deeply buried inside the active binding pocket of NiV-G protein which is constituted by highly conserved residues in the majority of the *Paramyxoviridae* family.

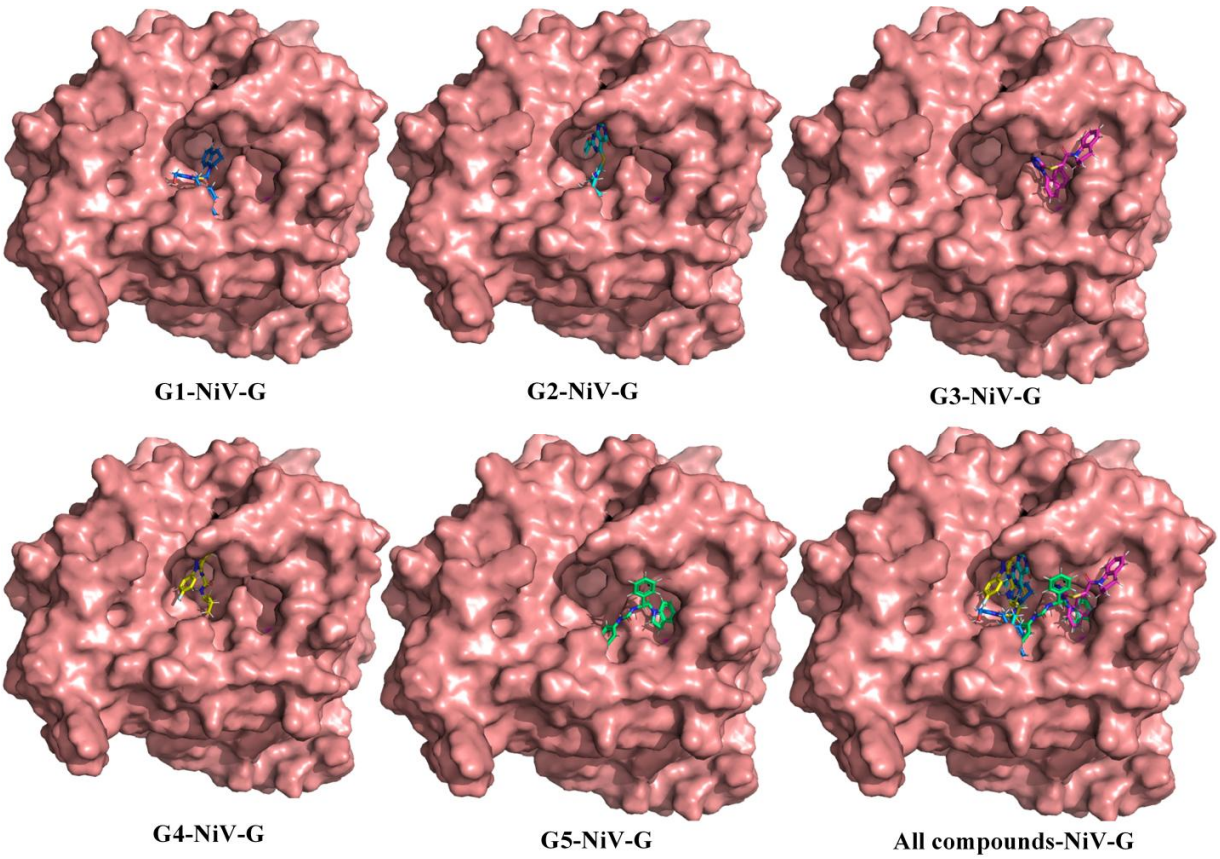

Figure 4. 3D surface view representation of molecular binding interaction of NiV-G protein with selected proposed five compounds (G1, G2, G3, G4 and G5).

Interestingly, the present study findings are highly corroborated with the earlier report where similar types of molecular docking interactions have been found between NiV-G protein and three studied compounds *viz*. MMV020537, MMV019838 and MMV688888 [35]. More precisely, the earlier study has demonstrated that a few amino acid residues such as Arg236, Cys240, His281, Pro441, Trp504, Tyr508, Ala532 and Lys560 of NiV-G protein implicated potential inter-molecular interactions with the three ligands mediated through H-bond and hydrophobic interactions [35]. Such observations undoubtedly favor the stability of the interaction of the NiV-G protein-ligand complex at the molecular level. The present study has

also revealed that all identified compounds displayed similar types of molecular recognition or interactions map for NiV-G protein. Moreover, in another study, the galectin-1-an endogenous lectin can bind to NiV-G protein directly and such binding inhibited the cell-cell fusion that was largely mediated by NiV-G [36]. In the current study, by close observations of the molecular binding orientations of all identified compounds with NiV-G protein, it can be postulated that G1 – G5 might possess some degree of direct and indirect mechanisms for inhibition of viral-mediated cell fusion and subsequently promotion of cytokine production.

3.3 In silico ADME and toxicity profile analyses of proposed NiV-G protein inhibitors

A number of ADMET parameters are considered to find out promising drug-like hit-to-lead compounds as NiV-G protein inhibitors. Precisely, different pharmacokinetics, physicochemical and toxicity properties have been predicted computationally in order to assess the drug-like chemical potentiality and toxicity or safety measures of all proposed NiV-G protein inhibitors. Results of all predicted pharmacokinetic and other ADME profiles of five proposed compounds are presented in Table 2. The molecular weight of G1, G2, G3, G4 and G5 is found to be 407.53, 451.5, 401.48, 390.43 and 385.46 g/mol, respectively. As per the recommendation of RoF, all proposed compounds follow the drug-likeness rule, as molecular weight accounted to be less than 500.00 g/mol. The relatively good or accepted oral activeness properties of many compounds can be explained by topological polar surface area (TPSA) which should be less than 140 $Å^2$. Herein, all proposed compounds have been found to have the TPSA score between 61.44 to 137.32 $Å^2$ which undoubtedly suggested that all compounds can be potentially orally active in nature.

Table 2. Predicted ADME and other pharmacokinetics profiles of selected five NiV-G inhibitors/modulators compounds.

Parameters	G1	G2	G3	G4	G5
[1]MW (g/mol)	407.53	451.5	401.48	390.43	385.46
[2]NHA	29	32	29	27	29
[3]NAHA	17	21	21	11	18
[4]NRB	7	8	5	7	7
[5]TPSA (Å^2)	83.66	137.32	89.21	110.55	61.44
[6]LogS	-4.88	-4.85	-6.41	-3.61	-5.11
[7]SC	Highly Soluble	Moderately Soluble	Soluble	Highly Soluble	Highly Soluble
[8]GI	High	High	High	High	High
[9]BBB	No	No	No	No	No
[10]vROF	0	0	0	0	0
[11]vGhose	0	0	0	0	0
[12]vVeber	0	0	0	0	0
[13]BS	0.55	0.55	0.55	0.55	0.55
[14]SA	3.23	3.4	3.01	3.9	3.34
iLOGp	2.69	3.17	3.46	2.91	3.64

[1]Molecular weight; [2]No.of heavy atoms; [3]No.of aromatic heavy atoms; [4]No. of rotatable bonds; [5]Topological polar surface area; [6]Solubility; [7]Solubility class; [8]Gastrointestinal absorption; [9]Blood Brain Barrier Penetration; [10]Violation of Lipinski's rule of five; [11]Violation of Ghose rule; [12]Violation of Veber rule; [13]Bioavailability Score; [14]Synthetic accessibility

The solubility potency of each compound has been predicted and found that all compounds possess moderately to highly soluble characteristics. Predicted human gastrointestinal absorption (GI) clearly indicates that each compound possesses high absorbable characteristics and hence of each compound can be highly absorbable in the intestine. The predicted synthetic accessibility score suggests that almost all proposed compounds are not difficult to synthesize. Moreover, the toxicity parameters prediction assessment also accounted to be safe in terms of several important toxicity properties. A number of toxicity properties of each molecule have been predicted through the TOPKAT. As per the prediction of TOPKAT tool, it has been found that all compounds (G1, G2, G3, G4 and G5) are non-mutagenic, non-

carcinogenic, non-toxic, non-irritant (as per values predicted for skin sensitization and skin irritancy), and non-ocular irritant. Undoubtedly, from the conceptual framework of interpretation among four irritancy levels - severe, moderate, mild, or non-irritant, all compounds have exhibited to be safe toxic class catergory.

Furthermore, the BOILED-EGG representation has been acquired from the data generated in the SwissADME web tool to analyze two other important parameters of the compounds such as HIA (Human Intestinal Absorption) and BBB (Blood-Brain Barrier). The pictorial diagram of BOILED-EGG predictions represents passive human gastrointestinal absorption (HIA) and blood-brain barrier (BBB) permeation (Figure 5). Particularly, the white region represents a high probability of passive absorption by the gastrointestinal tract, and the yellow region (yolk) represents a high probability of brain penetration. The predicted study results have revealed that the permeation ability of four compounds (G1, G2, G3 and G4) in albumin (white) and one compound (G5) in the yolk (yellow) region. The above findings have explained that four compounds that are in the white area more prone to penetrate the intestine and one compound found in the yolk area is believed to be capable of BBB. Further, it has been also observed that G1, G4 and G5 are effluent from the central nervous system (CNS) by P-Glycoprotein and which is marked as blue color in Figure 5. On the other hand, G2 and G3 are not effluent from CNS by P-Glycoprotein which is represented by red color. Overall, the predicted ADMET and other pharmacokinetic properties indicate that all five identified compounds can expedite drug discovery research for inhibiting or modulating the NiV-G protein function, however, all these compounds may need further optimization, based on experimental validation.

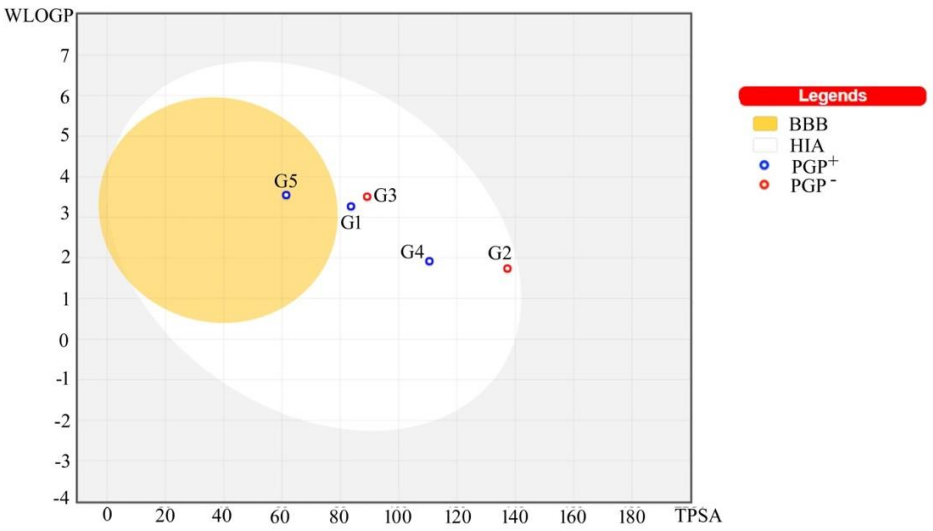

Figure 5. The EGG-BOILED model representation of the finally proposed NiV-G inhibitors/modulators

3.4 Molecular dynamic simulations analyses

MD simulation study has been performed to deduce an understanding of the behavior of the molecular interactions of the NiV-G binding protein with selected proposed ligand compounds to its dynamics state. Herein, a time-dependent interaction motion or behavior of NiV-G protein-ligand systems has been assessed through a classical MD simulation study. In particular, the MD simulation study has provided detailed information on fluctuation and structural or conformational changes of NiV-G protein and proposed compounds, and their inter or intra-atomic interactions for 100 ns time span. In order to analyze the stability or flexibility of each NiV-G protein-ligand complex, a number of parameters including RMSD, RMSF and RoG have been explored from the MD simulated trajectories. Usually, a significant impact in terms of assessing the quality of the MD simulations can be derived from these parameters. Precisely, the RMSD is calculated by rotating coordinates of the instantaneous structures by superimposing over the reference structure with maximum overlap. In the MD simulation study, RMSD is the measure of average changes in the displacement of a selection of atoms for a specific frame with respect to a reference frame. Such calculation can also be an indicator of the accuracy regarding the equilibration of any macromolecular systems and the occurrence of conformational changes in dynamic conditions. In this study, RMSD, RMSF and RoG measurements have been carried out based on the C_α atoms (protein backbone atoms) in the amino acid residues. On the other

hand, RMSF is a numerical measurement similar to RMSD but instead of indicating positional differences between entire structures over time, RMSF is a calculation of individual protein amino acid residue flexibility, or how much a particular residue fluctuates during a simulation. The higher protein backbone RMSF values indicate larger flexibility attained by the complex, whereas lower RMSF values indicate smaller flexibility for the complex [37]. RoG explicates the rigidity and compactness of any protein-ligand complex and it is the mass-weighted RMS (root-mean-square) distance of a collection of atoms from their common center derived from the MD simulation trajectories [37]. It is said that if a protein is stably folded, it will likely maintain a relatively steady value of RoG.

3.4.1 RMSD profile analyses of NiV-G protein-bound with proposed compounds

The RMSD of MD simulated NiV-G protein bound to each proposed compound has been depicted in Figure 6. The RMSD values of protein backbone atoms bound to each compound indicate that how protein backbone is internally existed and over time how it is changing structurally as compare to the starting point. Typically, the RMSD value less than 0.25 nm considered to be very close to the reference structure in terms of less occurrence of structural or conformational changes measured during the simulations. From Figure 6, it has been observed that fluctuations in RMSD values of simulated NiV-G protein backbone atoms are very less (<0.21 nm) for all compounds and thereby it can be suggested that conformational stability is achieved for the protein structure. The backbone RMSD of NiV-G protein-bound with compounds G1, G2, G3, G4, and G5 have been computed within the ranges of 0.00 to 0.21 nm. The minimum, maximum and average RMSD of NiV-G protein-bound with G1, G2, G3, G4, and G5 are presented in Table 3. The average RMSD of NiV-G protein has been found to be 0.147, 0.133, 0.155, 0.158 and 0.156 nm, respectively and these values indicate the greater stability of the NiV-G protein by means of the very smaller deviation observed in the protein backbone structure when attached with the selected proposed compounds. Mostly, a similar trend of RMSD fluctuations has been explicated in MD simulation for all compounds. From Figure 6, it can be observed that from the starting point all systems remain in the plateau state approximately till 50 ns. However, little fluctuations in RMSD values have shown afterward (~51 to 64 ns) increasing to RMSD value around 0.2 nm. Only NiV-G backbone bound with G5 has shown a sharp rise in RMSD value observed during ~ 41 to 64 ns. The highest protein

backbone RMSD found to be 0.22 nm when NiV-G is bound with G5. However, immediately thereafter the RMSD has achieved convergence near to the average and also progressing towards its equilibrium state and maintaining the same till the simulation ends. Undoubtedly, RMSD settles at lower values for all compounds when bound with NiV-G protein suggested that the convergence of the structure towards an equilibrium state. Likewise, similarities found in docking-based analyses reported by Georcki Ropón-Palacios *et al.* [35] and the performance of MD simulations also revealed very interesting RMSD profiles. Although, the above mentioned study has restricted the simulation time span up to only 40 ns, however, RMSD profile for compound MMV020537 implicated stable RMSD values as alike to the RMSD profiles of all compounds (G1 - G5) analyzed for 100 ns MD simulation run, in the present study. In an another study, where peptide-based NiV-G protein-FSPNLW inhibitor complex has been extensively studied for 100 ns MD simulation also demonstrated similar types of RMSD values nearer to the 0.2-0.3 nm throughout the simulation run [38]. Overall, observed low RMSD values of NiV-G protein backbone atoms indicates that all the systems remained stable during the MD simulation upon binding of the selected proposed compounds.

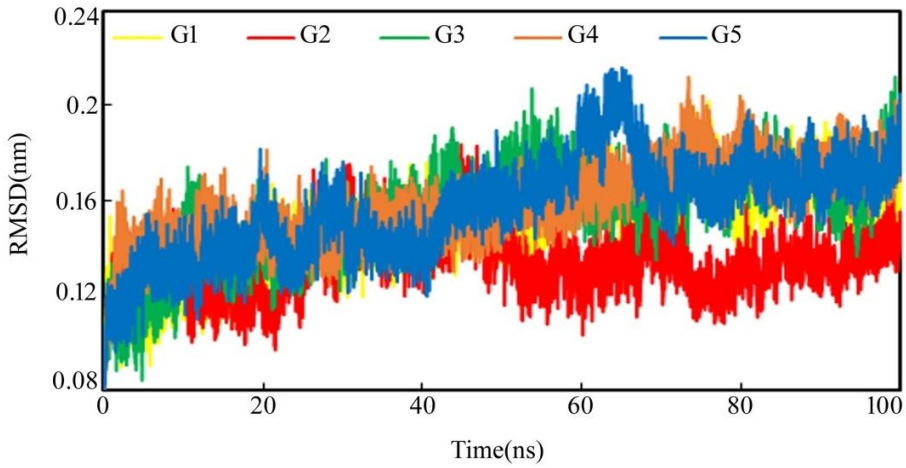

Figure 6. MD simulated protein backbone RMSD of NiV-G protein with the identified five compounds

3.4.2 RMSF profile analyses of NiV-G protein-bound with proposed compounds

The NiV-G protein backbone RMSF values plotted against each residue number during simulations is portrayed in Figure 7. The RMSF plot indicates that all compounds attached with NiV-G protein and each residue fluctuation has been measured within the 0.540 nm. The RMSF

parameter calculated from the MD simulation trajectories for each compound bound state and their maximum, minimum and average RMSF values are presented in Table 3. The differences between maximum and average RMSF values can give an idea about the overall RMSF fluctuation of the MD simulated system. It can be observed that amino acid residues approximately extending from 322 to 346 have fluctuated a bit higher for the G3 and G5 in comparison to others. Compound G2 bound with NiV-G protein has also shown slightly higher oscillation in RMSF values at residues 411 to 417 in comparison to the other region of the protein segment. Such fluctuations in RMSF values at that region of NiV-G protein has been earlier reported by Georcki Ropón-Palacios *et al.*[35]. These types of RMSF fluctuations in residue level can be expected because no compounds have been found to be associated to form any kind of molecular binding interaction at those protein segments. Otherwise, overall all five NiV-G protein-ligands (G1, G2, G3, G4 and G5) complexes disclosed a similar pattern of RMSF values during the entire simulation span. Fluctuations in RMSF values may also be observed due to structural organization of the NiV-G protein at residue level as well, however, the degree of flexibility in such a lower scale probably suggests no noticeable triggering effect or local changes along with the amino acid residues.

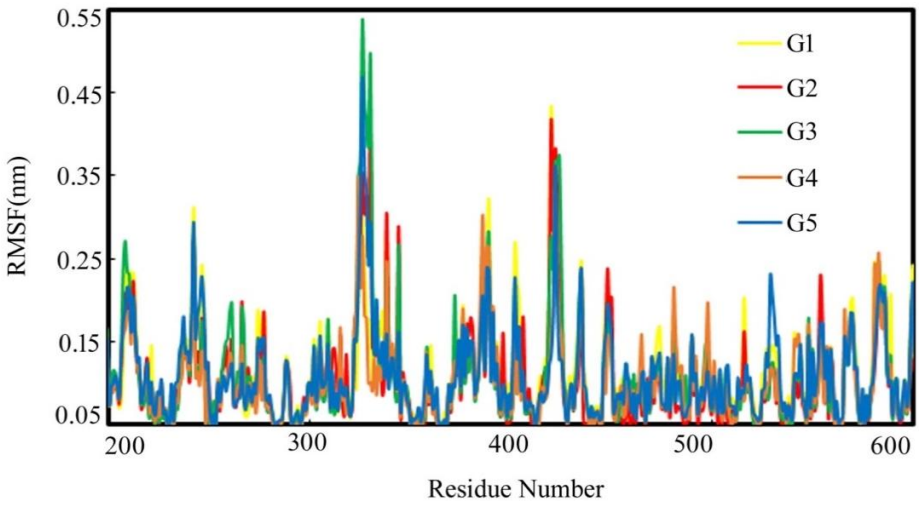

Figure 7. RMSF of amino acid residues in NiV-G protein observed during 100 ns MD simulations

3.4.3 RoG profile analyses of NiV-G protein bound with proposed compounds

The compound bound state of NiV-G protein structural compactness or folding organization of the simulated complexes has been assessed through another important parameter i.e. RoG. The

average RoG value for compounds G1, G2, G3, G4 and G5 has been measured as 2.123, 2.111, 2.127, 2.127 and 2.126 nm, respectively. The RoG value of each NiV-G frame bound with proposed molecules is plotted against time and it is depicted in Figure 8. From Figure 8, RoG value certainly demonstrated that all compounds bound with NiV-G protein complex stably folded throughout the simulation period, as no such observable fluctuations in RoG has been noticed. In particular, the NiV-G protein structure shows a similar pattern of RoG values with a low order of magnitude for the entire time span of MD simulations. Hence, it can be postulated that the binding of the proposed compounds is unable to disturb the structural organization of NiV-G protein during the dynamic condition. Overall, all compound bound NiV-G protein structures have exhibited quite consistent RoG values, which might indicate that all compounds bound protein stably folded and remained compact throughout the simulation run period. The minimum, maximum and average value of RoG have been calculated and presented in Table 3.

Table 3. Maximum, minimum and average RMSD, RMSF and RoG values for NiV-G protein backbone atoms of bound with five proposed compounds

		G1	**G2**	**G3**	**G4**	**G5**
RMSD (nm)	Minimum	0.001	0.001	0.001	0.001	0.001
	Maximum	0.202	0.183	0.212	0.212	0.216
	Average	0.147	0.133	0.155	0.158	0.156
RMSF (nm)	Minimum	0.046	0.042	0.041	0.041	0.046
	Maximum	0.437	0.438	0.537	0.373	0.486
	Average	0.116	0.107	0.112	0.104	0.120
RoG (nm)	Minimum	2.083	2.081	2.083	2.083	2.082
	Maximum	2.144	2.130	2.151	2.098	2.153
	Average	2.123	2.111	2.127	2.127	2.126

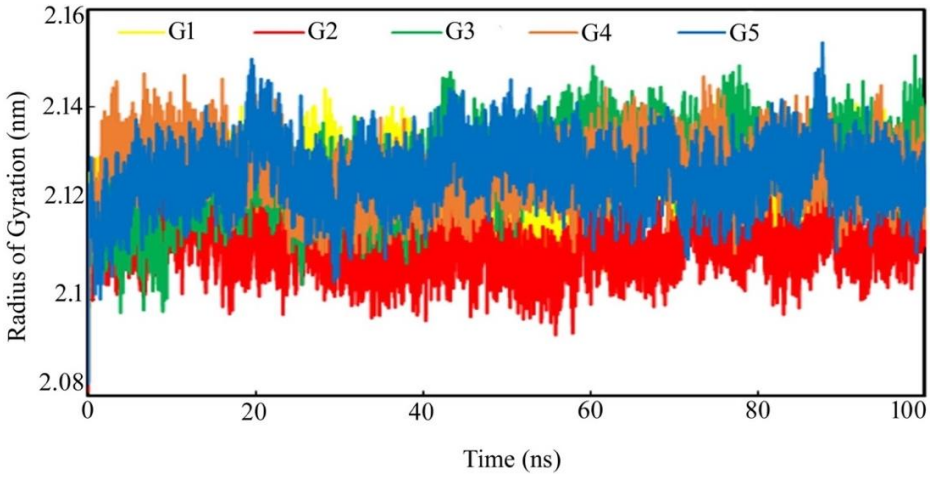

Figure 8. Radius of gyration (RoG) of NiV-G protein bound with the proposed compounds

3.5 Analyses of binding free energy estimation using MM-PBSA approach

The MM-PBSA based binding free energies (ΔG_{bind}) have been computed for all proposed identified compounds from 100 ns MD simulated trajectories obtained during simulation execution. The execution of MM-PBSA / MM-GBSA methodologies are quite computationally expensive and time-consuming too, however engaging such implicit solvation models for estimating the ΔG_{bind} value appears to be more accurate and reliable in comparison to other scoring algorithms [37, 39, 40]. Moreover, the ΔG_{bind} value can provide insight and understanding about the relative energy contribution of each proposed compound in maintaining and stabilizing the complex binding interactions with NiV-G protein. All estimated MM-PBSA based ΔG_{bind} values over time (ns) for complexes of NiV-G bound with five selected compounds are depicted in Figure 9. Among all five proposed compounds, it has been revealed that G2 has shown the highest average ΔG_{bind} value of -226.652 kJ/mol. The second-highest average ΔG_{bind} value (-216.859 kJ/mol) has been observed for G1. For G3, G4 and G5, the average ΔG_{bind} value has been found to be -166.246, -198.533 and -192.787 kJ/mol, respectively. The maximum, minimum and average ΔG_{bind} values are calculated for all compounds and presented in Table 4.

Table 4. Binding free energies of five proposed compounds

Compounds	G1	G2	G3	G4	G5
Minimum	-337.514	-372.990	-315.230	-308.187	-298.182
Maximum	-127.776	-79.580	-37.920	-35.803	-84.932
Average	-216.859	-226.652	-166.246	-198.533	-192.787
Std Deviation(±)	24.159	43.8718	46.0825	50.268	27.633

The interesting and noticeable fact accounted as throughout the simulation period all compounds have shown consistent energy contributions and there is no such higher fluctuation observed for any compounds, which suggests that all compounds can embrace its molecular interaction strongly with the NiV-G protein. Specifically, it has also been observed that electrostatic and van der Waals energy terms are two of the main energy contributing factors for the compound's binding interactions. Therefore, binding free energy analyses have clearly demonstrated that all compounds consist of important functional chemical features or components to form stable interactions with NiV-G protein. Such observations can explicate that all compounds have shown strong molecular binding attraction towards NiV-G protein for displaying essential biological action for inhibiting or modulating the function of NiV-G protein.

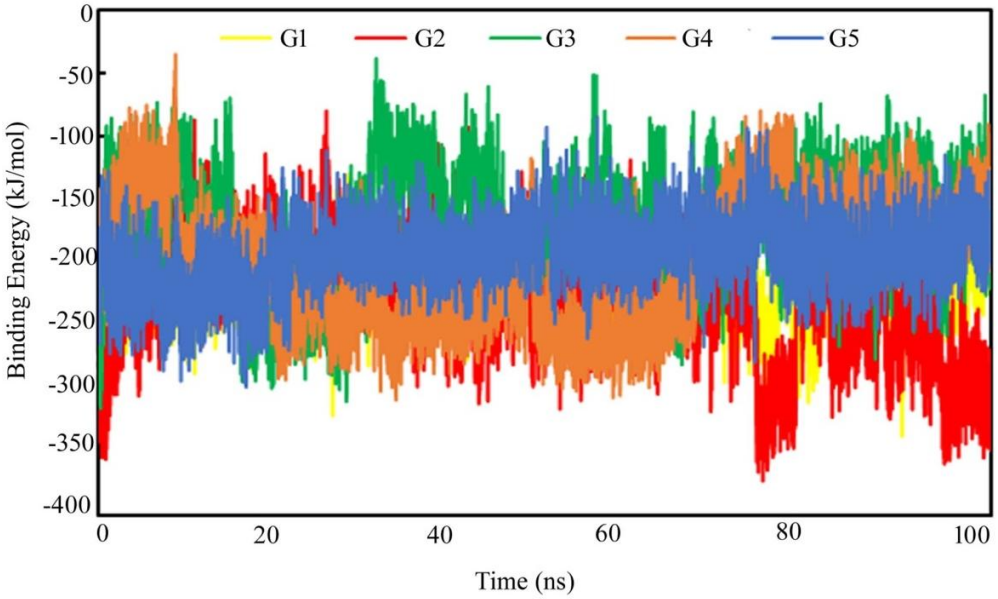

Figure 9. Computed MM-PBSA based binding free energies for complexes of NiV-G protein-bound with five proposed compounds

4. Conclusion

In this study, an extensive virtual screening has been carried out on specifically three large libraries of antiviral chemical databases for identifying potential inhibitors against NiV-G protein. Particularly, the study has been hypothesized to restrict the viral entry by means of modulating or inhibiting the NiV-G protein by small molecular chemical entities. Initially, using VSW protocol, three consecutive molecular docking procedures such as Glide-HTVS, Glide-SP, and Glide-XP have been executed to sequentially removing low potential compounds. Further, *in silico* pharmacokinetics properties analyses have been carried out on retained compounds for selection of best compounds consisting of good adsorption, distribution, metabolism and excretion characteristics. The toxic, mutagenic, irritant and carcinogenic compounds have been filtered out through the TOPKAT tool. Molecular binding interactions of retained compounds with NiV-G protein have been checked critically for the selection of potent NiV-G protein inhibitors/modulators. A long-range 100 ns MD simulation studies of NiV-G protein-ligand complexes have been executed to understand the stability of the complexes. The binding free energy has been calculated using the MM-PBSA approach from the MD simulation trajectories which suggested that all molecules possess a strong binding affinity towards NiV-G. After performing exhaustive analyses, the five best molecules were proposed as inhibitors/modulators for NiV-G protein. It can be concluded that the proposed molecules might be important to inhibit the NiV-G protein and subjected to experimental validation. Nevertheless, the limitation of the study can be accounted as not the availability of any standard compound as NiV-G protein inhibitor/modulator to further compared with the present study findings. Otherwise, any kind of experimental evaluation can provide insight into absolute molecular mechanisms of interaction of the identified compounds for modulating the biological effect of NiV-G protein. Since all identified compounds exhibited strong intermolecular interaction affinity towards NiV-G protein and hence may facilitate the possibility to be as promising drug-like candidates against NiV-G protein, however, may also need structural optimizations or valuable insights from extensive clinical testing for understanding host-pathogen interactions mechanisms.

Acknowledgment

This work was funded by the Researchers Supporting Project Number (RSP-2020/261) King Saud University, Riyadh, Saudi Arabia.

Computational resource
The CHPC (www.chpc.ac.za), Cape Town, South Africa is thankfully acknowledged for computational resources and tools.

Conflicts of interest/Competing interests
Authors declare that there is no competing interest

Availability of data and material
Not availability

References
[1] R.K. Plowright, D.J. Becker, D.E. Crowley, A.D. Washburne, T. Huang, P.O. Nameer, et al., Prioritizing surveillance of Nipah virus in India. PLoS Neglec Tropical Disease, 13 (2019) e0007393.
[2] L. Martinez-Gil, N.M. Vera-Velasco, I. Mingarro, Exploring the Human-Nipah Virus Protein-Protein Interactome, J Virol, 91 (2017).
[3] R.K. Singh, K. Dhama, S. Chakraborty, R. Tiwari, S. Natesan, R. Khandia, A. Munjal, K.S. Vora, S.K. Latheef, K. Karthik, Y. Singh Malik, R. Singh, W. Chaicumpa, D.T. Mourya, Nipah virus: epidemiology, pathology, immunobiology and advances in diagnosis, vaccine designing and control strategies - a comprehensive review, The veterinary quarterly, 39 (2019) 26-55.
[4] W.J. Bellini, B.H. Harcourt, N. Bowden, P.A. Rota, Nipah virus: an emergent paramyxovirus causing severe encephalitis in humans, Journal of neurovirology, 11 (2005) 481-487.
[5] K.B. Chua, W.J. Bellini, P.A. Rota, B.H. Harcourt, A. Tamin, S.K. Lam, T.G. Ksiazek, P.E. Rollin, S.R. Zaki, W. Shieh, C.S. Goldsmith, D.J. Gubler, J.T. Roehrig, B. Eaton, A.R. Gould, J. Olson, H. Field, P. Daniels, A.E. Ling, C.J. Peters, L.J. Anderson, B.W. Mahy, Nipah virus: a recently emergent deadly paramyxovirus, Science, 288 (2000) 1432-1435.
[6] P.A. Tambyah, J.H. Tan, B.K. Ong, K.H. Ho, K.P. Chan, First case of Nipah virus encephalitis in Singapore, Internal medicine journal, 31 (2001) 132-133.
[7] K.B. Chua, Nipah virus outbreak in Malaysia, Journal of clinical virology : the official publication of the Pan American Society for Clinical Virology, 26 (2003) 265-275.
[8] V.K. Chattu, R. Kumar, S. Kumary, F. Kajal, J.K. David, Nipah virus epidemic in southern India and emphasizing "One Health" approach to ensure global health security, Journal of family medicine and primary care, 7 (2018) 275-283.
[9] V. Sharma, S. Kaushik, R. Kumar, J.P. Yadav, Emerging trends of Nipah virus: A review, Reviews in medical virology, 29 (2019) e2010.
[10] Aditi, M. Shariff, Nipah virus infection: A review, Epidemiology and infection, 147 (2019) e95.
[11] K.T. Wong, W.J. Shieh, S. Kumar, K. Norain, W. Abdullah, J. Guarner, C.S. Goldsmith, K.B. Chua, S.K. Lam, C.T. Tan, K.J. Goh, H.T. Chong, R. Jusoh, P.E. Rollin, T.G. Ksiazek, S.R. Zaki, Nipah virus infection: pathology and pathogenesis of an emerging paramyxoviral zoonosis, The American journal of pathology, 161 (2002) 2153-2167.
[12] S. Erbar, A. Maisner, Nipah virus infection and glycoprotein targeting in endothelial cells, Virology journal, 7 (2010) 305.

[13] K.N. Bossart, M. Tachedjian, J.A. McEachern, G. Crameri, Z. Zhu, D.S. Dimitrov, C.C. Broder, L.F. Wang, Functional studies of host-specific ephrin-B ligands as Henipavirus receptors, Virology, 372 (2008) 357-371.
[14] T.A. Bowden, M. Crispin, D.J. Harvey, A.R. Aricescu, J.M. Grimes, E.Y. Jones, D.I. Stuart, Crystal Structure and Carbohydrate Analysis of Nipah Virus Attachment Glycoprotein: a Template for Antiviral and Vaccine Design, Journal of virology, 82 (2008) 11628-11636.
[15] A. Garcia-Garcia, J. Galvez, J.V. de Julian-Ortiz, R. Garcia-Domenech, C. Munoz, R. Guna, R. Borras, New agents active against Mycobacterium avium complex selected by molecular topology: a virtual screening method, The Journal of antimicrobial chemotherapy, 53 (2004) 65-73.
[16] E. Harder, W. Damm, J. Maple, C. Wu, M. Reboul, J.Y. Xiang, L. Wang, D. Lupyan, M.K. Dahlgren, J.L. Knight, J.W. Kaus, D.S. Cerutti, G. Krilov, W.L. Jorgensen, R. Abel, R.A. Friesner, OPLS3: A Force Field Providing Broad Coverage of Drug-like Small Molecules and Proteins, Journal of Chemical Theory and Computation, 12 (2016) 281-296.
[17] H.M. Berman, J. Westbrook, Z. Feng, G. Gilliland, T.N. Bhat, H. Weissig, I.N. Shindyalov, P.E. Bourne, The Protein Data Bank, Nucleic acids research, 28 (2000) 235-242.
[18] T.A. Bowden, A.R. Aricescu, R.J. Gilbert, J.M. Grimes, E.Y. Jones, D.I. Stuart, Structural basis of Nipah and Hendra virus attachment to their cell-surface receptor ephrin-B2, Nature structural & molecular biology, 15 (2008) 567-572.
[19] P. Kirubakaran, K. Muthusamy, K.H. Singh, S. Nagamani, Ligand-based Pharmacophore Modeling; Atom-based 3D-QSAR Analysis and Molecular Docking Studies of Phosphoinositide-Dependent Kinase-1 Inhibitors, Indian journal of pharmaceutical sciences, 74 (2012) 141-151.
[20] G. Madhavi Sastry, M. Adzhigirey, T. Day, R. Annabhimoju, W. Sherman, Protein and ligand preparation: parameters, protocols, and influence on virtual screening enrichments, J Comput Aided Mol Des, 27 (2013) 221-234.
[21] S. Pathania, V. Randhawa, M. Kumar, Identifying potential entry inhibitors for emerging Nipah virus by molecular docking and chemical-protein interaction network, Journal of Biomolecular Structure and Dynamics, 38 (2020) 5108-5125.
[22] V. Law, C. Knox, Y. Djoumbou, T. Jewison, A.C. Guo, Y. Liu, A. Maciejewski, D. Arndt, M. Wilson, V. Neveu, A. Tang, G. Gabriel, C. Ly, S. Adamjee, Z.T. Dame, B. Han, Y. Zhou, D.S. Wishart, DrugBank 4.0: shedding new light on drug metabolism, Nucleic acids research, 42 (2014) D1091-1097.
[23] A. Daina, O. Michielin, V. Zoete, SwissADME: a free web tool to evaluate pharmacokinetics, drug-likeness and medicinal chemistry friendliness of small molecules, Scientific reports, 7 (2017) 42717.
[24] H.J.C. Berendsen, D. van der Spoel, R. van Drunen, GROMACS: A message-passing parallel molecular dynamics implementation, Computer Physics Communications, 91 (1995) 43-56.
[25] C. Kutzner, S. Páll, M. Fechner, A. Esztermann, B.L. de Groot, H. Grubmüller, More bang for your buck: Improved use of GPU nodes for GROMACS 2018, J Comput Chem, 40 (2019) 2418-2431.
[26] R. Kumari, R. Kumar, A. Lynn, g_mmpbsa—A GROMACS Tool for High-Throughput MM-PBSA Calculations, Journal of chemical information and modeling, 54 (2014) 1951-1962.

[27] P.B. Shinde, S. Bhowmick, E. Alfantoukh, P.C. Patil, S.M. Wabaidur, R.V. Chikhale, M.A. Islam, De novo design based identification of potential HIV-1 integrase inhibitors: A pharmacoinformatics study, Computational biology and chemistry, 88 (2020) 107319.
[28] S. Gupta, D. Parihar, M. Shah, S. Yadav, H. Managori, S. Bhowmick, P.C. Patil, S.A. Alissa, S.M. Wabaidur, M.A. Islam, Computational screening of promising beta-secretase 1 inhibitors through multi-step molecular docking and molecular dynamics simulations - Pharmacoinformatics approach, Journal of Molecular Structure, 1205 (2020) 127660.
[29] S. Bhowmick, K. Roy, A. Saha, Exploring CIP2A modulators using multiple molecular modeling approaches, J Biomol Struct Dyn, (2020) 1-16.
[30] Y. Haddad, M. Remes, V. Adam, Z. Heger, Toward structure-based drug design against the epidermal growth factor receptor (EGFR), Drug Discovery Today, (2020).
[31] E. Lionta, G. Spyrou, D.K. Vassilatis, Z. Cournia, Structure-based virtual screening for drug discovery: principles, applications and recent advances, Current topics in medicinal chemistry, 14 (2014) 1923-1938.
[32] I. Kuriwaki, M. Kameda, H. Hisamichi, S. Kikuchi, K. Iikubo, Y. Kawamoto, H. Moritomo, Y. Kondoh, Y. Amano, Y. Tateishi, Y. Echizen, Y. Iwai, A. Noda, H. Tomiyama, T. Suzuki, M. Hirano, Structure-based drug design of 1,3,5-triazine and pyrimidine derivatives as novel FGFR3 inhibitors with high selectivity over VEGFR2, Bioorganic & Medicinal Chemistry, 28 (2020) 115453.
[33] L.G. Ferreira, R.N. Dos Santos, G. Oliva, A.D. Andricopulo, Molecular docking and structure-based drug design strategies, Molecules, 20 (2015) 13384-13421.
[34] S. Salentin, S. Schreiber, V.J. Haupt, M.F. Adasme, M. Schroeder, PLIP: fully automated protein-ligand interaction profiler, Nucleic acids research, 43 (2015) W443-447.
[35] G. Ropon-Palacios, M.E. Chenet-Zuta, G.E. Olivos-Ramirez, K. Otazu, J. Acurio-Saavedra, I. Camps, Potential novel inhibitors against emerging zoonotic pathogen Nipah virus: a virtual screening and molecular dynamics approach, J Biomol Struct Dyn, 38 (2020) 3225-3234.
[36] E.L. Levroney, H.C. Aguilar, J.A. Fulcher, L. Kohatsu, K.E. Pace, M. Pang, K.B. Gurney, L.G. Baum, B. Lee, Novel innate immune functions for galectin-1: galectin-1 inhibits cell fusion by Nipah virus envelope glycoproteins and augments dendritic cell secretion of proinflammatory cytokines, J Immunol, 175 (2005) 413-420.
[37] S. Bhowmick, N.A. AlFaris, J.Z. Altamimi, Z.A. Alothman, T.S. Aldayel, S.M. Wabaidur, M.A. Islam, Screening and analysis of bioactive food compounds for modulating the CDK2 protein for cell cycle arrest: Multi-cheminformatics approaches for anticancer therapeutics, Journal of Molecular Structure, 1216 (2020) 128316.
[38] N. Sen, T.R. Kanitkar, A.A. Roy, N. Soni, K. Amritkar, S. Supekar, S. Nair, G. Singh, M.S. Madhusudhan, Predicting and designing therapeutics against the Nipah virus, PLoS neglected tropical diseases, 13 (2019) e0007419.
[39] P.P. Dike, S. Bhowmick, G.E. Eldesoky, S.M. Wabaidur, P.C. Patil, M.A. Islam, In silico identification of small molecule modulators for disruption of Hsp90-Cdc37 protein-protein interaction interface for cancer therapeutic application, J Biomol Struct Dyn, (2020) 1-17.
[40] S. Bhowmick, S.A. Alissa, S.M. Wabaidur, R.V. Chikhale, M.A. Islam, Structure-guided screening of chemical database to identify NS3-NS2B inhibitors for effective therapeutic application in dengue infection, Journal of molecular recognition : JMR, 33 (2020) e2838.